Molecular Therapy
Original Article

Targeting RNA editing of *antizyme inhibitor 1*: A potential oligonucleotide-based antisense therapy for cancer

Daryl Jin Tai Tay,[1] Yangyang Song,[1] Boya Peng,[2,3] Tan Boon Toh,[1,4] Lissa Hooi,[1] Desiree-Faye Kaixin Toh,[5] HuiQi Hong,[1,6] Sze Jing Tang,[1] Jian Han,[1] Wei Liang Gan,[1] Tim Hon Man Chan,[1] Manchugondanahalli S. Krishna,[5] Kiran M. Patil,[5] Manikantha Maraswami,[5] Teck Peng Loh,[5] Yock Young Dan,[1,7] Lei Zhou,[7] Glenn Kunnath Bonney,[8,9] Pierce Kah-Hoe Chow,[10,11,12] Gang Chen,[5,13] Edward Kai-Hua Chow,[1,2,4,9] Minh T.N. Le,[2,3] and Leilei Chen[1,9,14]

[1]Cancer Science Institute of Singapore, National University of Singapore, 14 Medical Drive, Singapore 117599, Singapore; [2]Department of Pharmacology, Yong Loo Lin School of Medicine, National University of Singapore, 16 Medical Drive, Singapore 117600, Singapore; [3]Department of Biomedical Sciences, School of Veterinary Medicine and Life Sciences, City University of Hong Kong, 83 Tat Chee Avenue, Kowloon, Hong Kong; [4]The N.1 Institute for Health (N.1), 28 Medical Drive, Singapore 117456, Singapore; [5]Division of Chemistry and Biological Chemistry, School of Physical and Mathematical Sciences, Nanyang Technological University, Singapore, 21 Nanyang Link, Singapore 637371, Singapore; [6]Department of Physiology, Yong Loo Lin School of Medicine, National University of Singapore, 2 Medical Drive, Singapore 117593, Singapore; [7]Division of Gastroenterology and Hepatology, National University Health System, Singapore 119228, Singapore; [8]Division of Hepatobiliary and Liver Transplantation Surgery, National University Health System, Singapore 119228, Singapore; [9]NUS Center for Cancer Research, Yong Loo Lin School of Medicine, National University Singapore, Singapore, Singapore 117594, Singapore; [10]Division of Surgical Oncology, National Cancer Centre Singapore, Singapore 169610, Singapore; [11]Department of Hepato-Pancreato-Biliary and Transplant Surgery, Singapore General Hospital, Singapore 169608, Singapore; [12]Duke-NUS Medical School, Singapore 169857, Singapore; [13]School of Life and Health Sciences, The Chinese University of Hong Kong, Shenzhen (CUHK-Shenzhen), Shenzhen, Guangdong 518172, P. R. China; [14]Department of Anatomy, Yong Loo Lin School of Medicine, National University of Singapore, 4 Medical Drive, Singapore 117594, Singapore

Dysregulated adenosine-to-inosine (A-to-I) RNA editing is implicated in various cancers. However, no available RNA editing inhibitors have so far been developed to inhibit cancer-associated RNA editing events. Here, we decipher the RNA secondary structure of *antizyme inhibitor 1* (*AZIN1*), one of the best-studied A-to-I editing targets in cancer, by locating its editing site complementary sequence (ECS) at the 3′ end of exon 12. Chemically modified antisense oligonucleotides (ASOs) that target the editing region of *AZIN1* caused a substantial exon 11 skipping, whereas ECS-targeting ASOs effectively abolished *AZIN1* editing without affecting splicing and translation. We demonstrate that complete 2′-*O*-methyl (2′-*O*-Me) sugar ring modification in combination with partial phosphorothioate (PS) backbone modification may be an optimal chemistry for editing inhibition. ASO3.2, which targets the ECS, specifically inhibits cancer cell viability *in vitro* and tumor incidence and growth in xenograft models. Our results demonstrate that this *AZIN1*-targeting, ASO-based therapeutics may be applicable to a wide range of tumor types.

INTRODUCTION

RNA editing is a widespread co- or post-transcriptional modification process that introduces changes in RNA sequences encoded by the genome, contributing to "RNA mutations." Editing of adenosine to inosine (A to I) in double-stranded RNA (dsRNA), catalyzed by the adenosine deaminase acting on RNA (ADAR) family of enzymes, is the most common type of RNA editing in mammals.[1] In vertebrates, a family of 3 ADAR proteins, ADAR1, ADAR2, and ADAR3, has been characterized.[2] ADAR1 and ADAR2 (ADARs) catalyze all currently known A-to-I editing events. In contrast, ADAR3 has no documented deaminase activity. Inosine essentially mimics guanosine (G); therefore, ADAR proteins introduce a virtual A-to-G substitution in transcripts. Such changes can lead to specific amino acid substitutions,[3–8] alternative splicing,[9] microRNA-mediated gene silencing,[10,11] or changes in transcript localization and stability.[12–14]

Aberrant editing on specific transcripts and their association with cancer progression have been discovered in many cancer types.[15–17] The protein-recoding type of RNA editing contributes to tumorigenesis mainly through enhancing the activity of oncogenes or reducing the activity of tumor suppressors.[3,18–21] *AZIN1* (antizyme inhibitor 1) is one of the best-studied ADAR1 targets in cancer. Editing of *AZIN1* results in a serine (S) to glycine (G) substitution at residue 367, and the edited form AZIN1^{S367G} is more stable and has a stronger affinity

Received 14 September 2020; accepted 5 May 2021;
https://doi.org/10.1016/j.ymthe.2021.05.008.

Correspondence: Leilei Chen, Cancer Science Institute of Singapore, National University of Singapore, 14 Medical Drive, Singapore 117599, Singapore.
E-mail: polly_chen@nus.edu.sg

to antizyme (AZ) than AZIN1$^{wild\text{-}type}$. AZ binds and degrades proteins associated with cell growth and proliferation such as ornithine decarboxylase (ODC) and cyclin D1 (CCND1). AZIN1^{S367G} inhibits AZ-mediated degradation of ODC and CCND1 by competing with AZIN1$^{wild\text{-}type}$ for binding to AZ, thereby facilitating entry into cell cycle and possessing much stronger tumorigenic capabilities than AZIN1$^{wild\text{-}type}$. Importantly, RNA editing level of *AZIN1* is significantly higher in different cancer types such as hepatocellular carcinoma (HCC),[3] esophageal squamous cell carcinoma (ESCC),[4] non-small-cell lung cancer (NSCLC),[6] and colorectal cancer (CRC)[5] compared with corresponding non-cancerous tissues. Elevated editing frequency of *AZIN1* has also emerged as a prognostic factor for overall survival and disease-free survival and an independent risk factor for lymph node and distant metastasis.[5] All these findings strongly suggest that suppressing *AZIN1* editing may contribute to the development of novel RNA therapies for cancer treatment.

Unfortunately, RNA therapeutics targeting cancer-driven or associated RNA editing events have not yet been identified or introduced into the clinic. In this study, we employed chemically modified antisense oligonucleotides (ASOs) to sensitively and specifically inhibit *AZIN1* editing. ASOs can be defined as single- or double-stranded oligonucleotides, ~15–25 nucleotides (nt) in length, that can bind to RNA through Watson-Crick base pairing. In an effort to increase cellular uptake, stability, target binding affinity, and specificity while reducing nuclease cleavage and immune response from TLRs (Toll-like receptors), backbone modifications (e.g., phosphodiester, phosphorothioate [PS]), and sugar ring modifications such as 2′-*O*-Me (2′-*O*-methyl), 2′-*O*-MOE (2′-methoxyethyl), and locked nucleic acid (LNA) have been widely used for ASOs. To confer site-specific RNA editing inhibition, ASOs must be able to enter the cell nucleus and sequester or block ADAR proteins from binding to target RNAs. They must also not trigger RNase H or RNA interference (RNAi) response against RNA targets. To date, ASOs containing 2′-*O*-Me or 2′-*O*-MOE in combination with the PS backbone modification, or highly modified ASOs including phosphorodiamidate morpholino oligomer (PMO) and peptide nucleic acid (PNA), have been utilized to modulate splicing and inhibit translation.[22–24] However, for RNA editing inhibition, very few studies showed that morpholino ASO and 2′-*O*-Me/LNA-modified ASOs were capable of inhibiting editing of certain targets with low or modest potency, such as the Q/R site of *GluA2*[25] (glutamate ionotropic receptor AMPA type subunit 2), *HTR2C*[26](5-hydroxytryptamine receptor 2C), and *NEIL1*[26] (Nei like DNA glycosylase 1)

In this study, we applied a minigene system to uncover the editing site complementary sequence (ECS) of *AZIN1* that forms dsRNA with the editing region at exon 11, which allows ADAR1 protein to bind and catalyze the deaminase reaction. Based on this finding, we designed and synthesized PNAs, 2′-*O*-Me alone, or 2′-*O*-Me/PS-modified ASOs that target either the editing region or the ECS and evaluated their potential to inhibit *AZIN1* editing and cancer cell viability *in vitro* and *in vivo*. We found that complete 2′-*O*-Me sugar ring modification in combination with partial PS backbone modification may be an optimal chemistry for RNA editing inhibition, and ASOs that target the ECS, but not the editing region, could effectively abolish *AZIN1* editing without affecting splicing and translation. 2′-*O*-Me/PS-modified ASO3.2, which targets the ECS, specifically inhibits the viability of cancer cell lines as well as cells derived from HCC patient-derived xenografts (PDXs) *in vitro* and tumor incidence and growth in xenograft models. Altogether, our study develops an ASO-based RNA editing inhibitor and provides an attractive approach for targeting cancer-associated RNA editing substrates. The delivery of therapeutically effective, chemically stabilized ASOs into human liver and central nervous system (CNS) has been achieved recently,[27] suggesting that developing an ASO-based RNA editing inhibitor of *AZIN1* may hold great promise for the treatment of cancer, particularly liver cancer.

RESULTS

An 8-nt sequence at 3′ end of exon 12 is the core ECS and indispensable for *AZIN1* editing

Uncovering the ECS of *AZIN1* transcript would help to decipher the precise dsRNA structure, which is essential for *AZIN1* editing. To this end, *AZIN1* minigene constructs were generated by inserting fragments of different length covering the edited exon 11 and flanking exons and introns into either pRK7 or pcDNA3.1 vector (Figure 1A). *HTR2C*, which is a well-characterized editing target with its dsRNA structure well delineated in many studies,[28–30] was used to generate *HTR2C* minigene as a positive control. Upon co-transfection of the *HTR2C* minigene and *ADAR1* expression construct, ~75.8% of endogenous *AZIN1* was edited, indicating a successful ADAR1 overexpression (Figure 1B, left; Figure S1). Moreover, three known editing sites were detected in exogenous *HRT2C* transcripts (Figure 1B, right), supporting the feasibility of using the pRK7 minigene system in this study. Among all *AZIN1* minigenes, only *AZIN1* transcripts transcribed from the minigene containing fragment A (FA), which lacks a 90-bp sequence at the 3′ end of exon 12, was unable to be edited (Figures 1A and 1C). This observation could be confirmed by using pcDNA3.1-based minigenes, ruling out the possibility of artifacts of the pRK7 minigene system (Figure 1D). These findings suggested that the ECS is most likely to be at the 3′ end of exon 12.

To precisely locate the ECS, RNA sequence corresponding to fragment E (FE) was used for secondary structure prediction by RNAfold.[31] Of note, the 3′ end of exon 12 forms dsRNA with the edited sequence (Figure 1E). FE minigene was utilized to generate 3 additional minigenes by deleting a 29-bp sequence at the 3′ end of exon 12 (FE-1) or introducing an 8-bp internal deletion (FE-2) or point mutations (FE-3) into the potential ECS (Figure 2A). As predicted by RNAfold, both deletion and mutations dramatically alter the dsRNA structure (Figure 2B). Using the same strategy described above, we observed that transcripts transcribed from FE-1, -2, and -3 were not edited upon ADAR1 overexpression (Figure 2C; Figure S2). Further, *in vitro* RNA editing analysis showed that *AZIN1* transcripts transcribed from FB or FE, but not FA, FE-2, and FE-3, could be edited in the presence of purified ADAR1 protein (Figure 2D). All these data supported that an 8-nt sequence (5′-

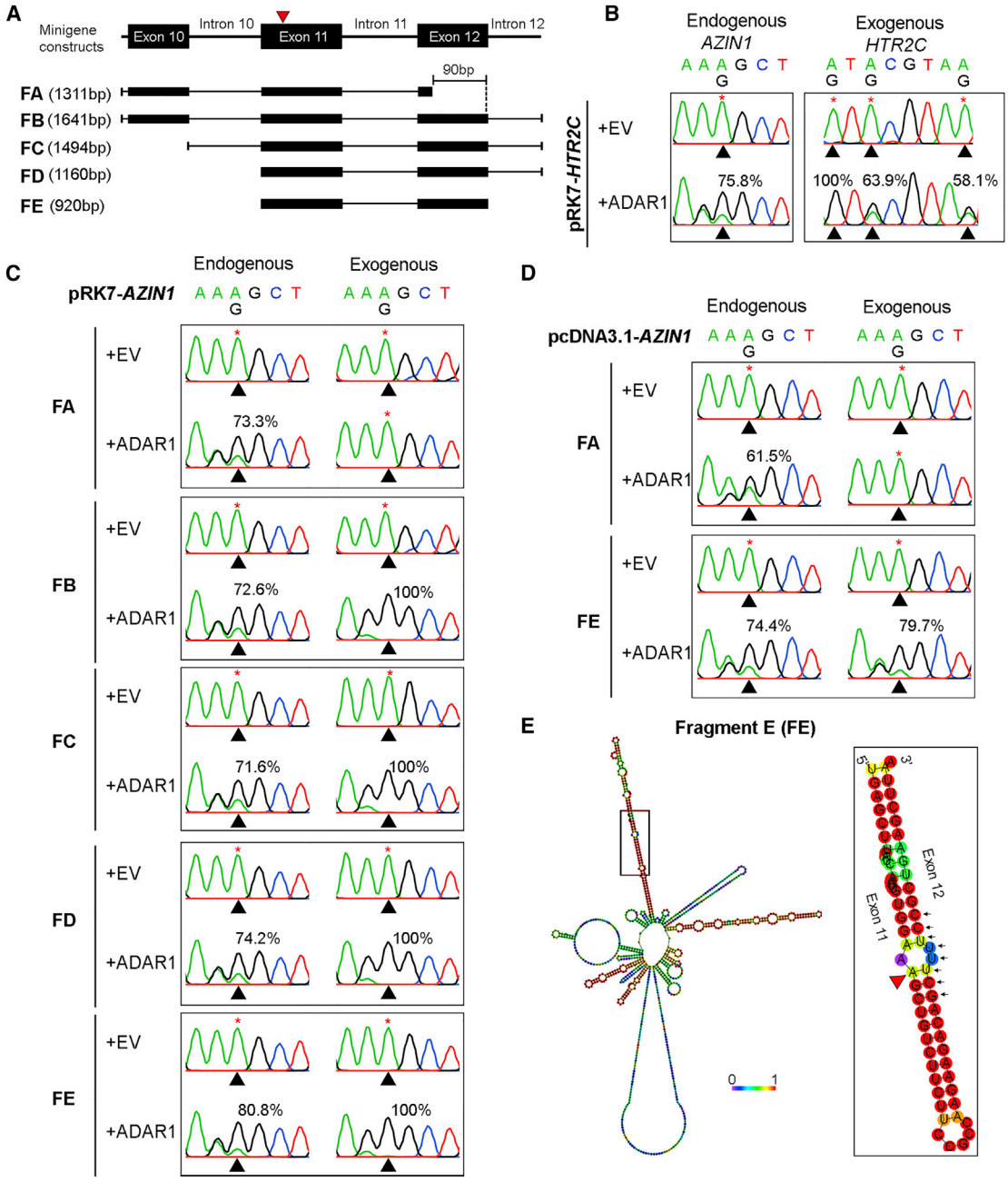

Figure 1. The 3′ end sequence of exon 12 is required for *AZIN1* editing

(A) Schematic diagram of *AZIN1* minigene constructs generated by inserting five different fragments (FA, FB, FC, FD, or FE) covering the edited exon 11 and flanking exons (exons 10 and 12) and introns (introns 9, 10, 11, and 12) into either pRK7 or pcDNA3.1 vector. Red arrow indicates relative position of the editing site. (B and C) Sequencing chromatograms illustrate editing of endogenous *AZIN1* (B, left) and exogenous *HTR2C* (B, right) or *AZIN1* (C) transcripts transcribed from pRK7-based minigene constructs in the HEK293T cells co-transfected with the indicated pRK7 minigenes and empty vector (EV) or ADAR1 expression construct (ADAR1). (D) Sequencing chromatograms illustrate editing of endogenous and exogenous *AZIN1* transcripts in HEK293T cells co-transfected with pcDNA3.1-based minigenes and EV or ADAR1. (E) Predicted dsRNA structure of *AZIN1* by RNAfold. An 8-nt sequence indicated by black arrows is the potential core ECS. Editing site is indicated by red arrowhead. Base pair probabilities are shown by a color spectrum. (B–D) Percentage of editing is calculated as area of "G" peak over the total area of "A" and "G" peaks. *, no editing detected. Black arrow indicates the position of editing site.

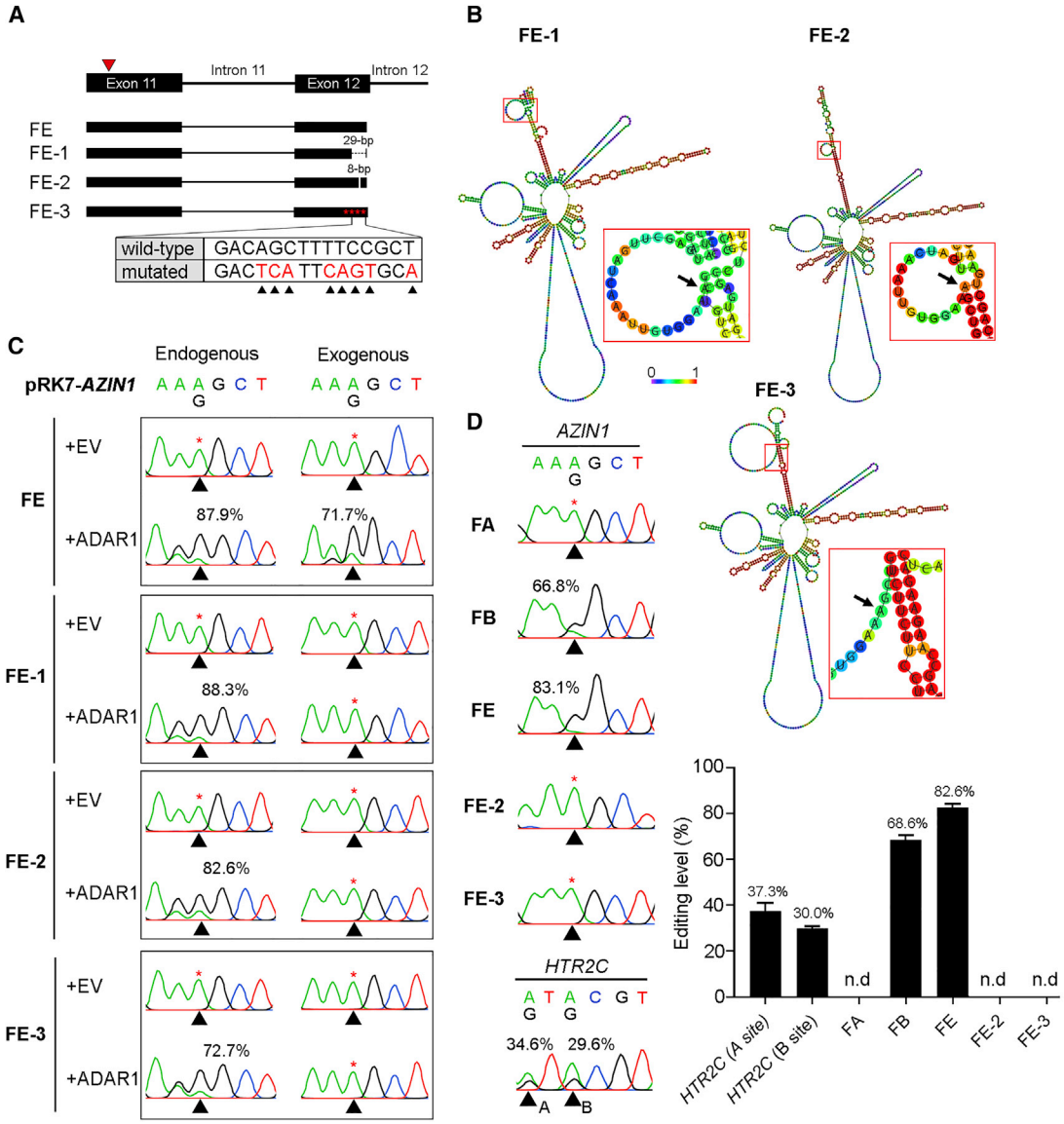

Figure 2. An 8-nt sequence at the 3′ end of exon 12 is the core ECS and indispensable for *AZIN1* editing

(A) Schematic diagram of FE-1, -2, and -3 minigene constructs. Black arrowheads indicate the mutations introduced into FE-3 minigene. Red arrow indicates the position of the editing site. (B) Predicted dsRNA structure of *AZIN1* transcribed from the indicated minigene by RNAfold. Black arrow indicates the editing site. Base pair probabilities are shown by a color spectrum. (C) Sequencing chromatograms illustrate editing of endogenous and exogenous *AZIN1* transcripts in HEK293T cells co-transfected with pRK7-based minigenes and EV or ADAR1. (D) *In vitro* RNA editing analysis of *AZIN1* transcripts. Left: *in vitro* transcribed *HTR2C* or *AZIN1* transcripts from the indicated minigene construct were incubated with purified ADAR1 protein, followed by RNA editing analysis using Sanger sequencing. *In vitro* transcribed *HTR2C* serves as a positive control. Right: data are presented in the bar chart as the mean ± SD of technical triplicates from a representative experiment of 3 independent experiments. n.d., not detectable. (C and D) Percentage of editing is calculated as area of "G" peak over the total area of "A" and "G" peaks. *, no editing detected. Black arrow indicates the position of editing site.

GCUUUUCC-3′) at the 3′ end of exon 12 is the core ECS and indispensable for dsRNA formation and *AZIN1* editing.

Identifying ASOs with pronounced *in vitro* editing inhibitory effects

Based on the elucidation of the *AZIN1* dsRNA, 7 entirely 2′-*O*-Me-modified ASOs (ASO1, ASO5, ASO6, and ASO7 target the editing region, and ASO2, ASO3, and ASO4 target the ECS region), an antisense PNA (ASP1), and 2 dsRNA-binding PNAs (DSP1 and DSP2) were designed and synthesized (Figure 3A; Table S1). As negative controls, 4 ASOs were designed, including ASO-ctl (6 point mutations were introduced into ASO2), ASO-ctl1, ASO-ctl2, and ASO-ctl3 (share the same sequence with ASO3 except carrying one, double, and triple point mutations, respectively) (Figure 3A). The *AZIN1*

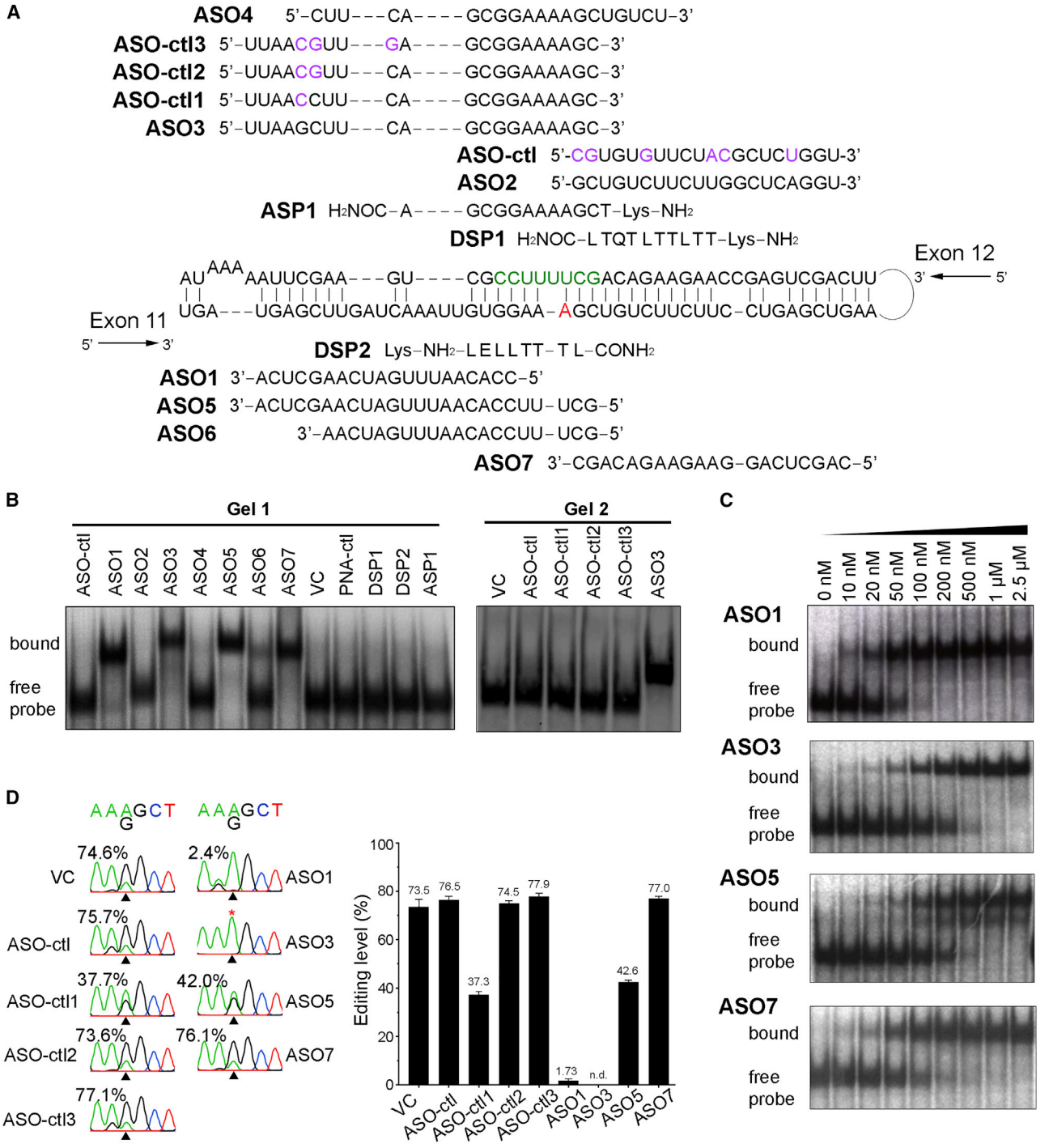

Figure 3. Screening of effective ASOs that can bind to *AZIN1* duplex and inhibit *AZIN1* editing *in vitro*

(A) Illustration of the design of ASOs. A short RNA duplex containing the editing region consisting of partial exon 11 with the edited adenosine (highlighted in red) and partial exon 12 containing the ECS region (the 8-nt core ECS is highlighted in green) is used for designing ASOs that target either the editing or ECS region. Point mutations introduced into each control ASO are highlighted in purple. Sequences of each oligo and their characteristics are listed in Table S1. (B) REMSA was performed to examine the binding of each ASO (2.5 μM) to ^{32}P-labeled *AZIN1* RNA duplexes (86 nt in length). The sequence and predicted secondary structure of the duplex probe are listed in Table S3, Figure 3A, and Figure S3A. Vehicle control (VC), no ASO added. (C) Binding of ASO1, 3, 5, or 7 to the duplexes described in (B) was detected by REMSA, at different

(legend continued on next page)

RNA duplex was designed with the use of RNAfold to cover both the editing region and the ECS region (Figure S3A). Binding of each oligo to the *AZIN1* RNA duplex was examined by RNA electrophoretic mobility shift assay (REMSA) (Figure 3B; Figure S3B). We observed a strong band shift in the presence of ASO1, ASO3, ASO5, and ASO7, whereas very weak or no shift was detected upon the addition of ASO2, ASO4, ASO6, all 3 PNAs, and 4 control ASOs (Figure 3B). Further, with increasing amounts of ASO1, 3, 5, or 7 added, a dose-dependent increase in the amount of shifted duplex probe was detected, confirming the binding capability of these ASOs to *AZIN1* with sub-micromolar affinity (Figure 3C). Because PNAs are shorter than ASOs, further testing using a shortened *AZIN1* probe showed that ASP1 (12-mer) remains incapable of binding to the *AZIN1* duplex, whereas DSP1 and DSP2 could bind through PNA-dsRNA triplex formation with a modest binding affinity (Figure S3B, micromolar).

Next, to examine whether the binding of each oligo to the *AZIN1* duplex is sufficient to inhibit *AZIN1* editing, ASO1, 3, 5, and 7 and control ASOs were used in *in vitro* editing assays. With the addition of ASO3, *AZIN1* editing was completely abolished; compared to ASO3, ASO1 was slightly less effective but repressed editing from 75.7% to 2.4%; and ASO5 and ASO7 demonstrated minor and no inhibition, respectively (Figure 3D). All control ASOs except ASO-ctl1 were unable to inhibit *AZIN1* editing *in vitro*. As seen in Figure S4, a weak binding of ASO-ctl1 to the *AZIN1* duplex probe was observed when we added 10-fold more ASO-ctl1. We therefore excluded ASO-ctl1 from the following experiments. Surprisingly, even though ASO5 could directly target the editing site because of an additional 5 nucleotides (GCUUU) on the 5′ end of ASO1 (Figure 3A), it failed to improve or maintain the editing inhibitory effect of ASO1, consistent with the fact that ASO5 has a slightly weakened binding compared with ASO1 (Figure 3C). This is probably because the base pairs involving the edited sequence (AAAGC) (potentially 3 A-U and 2 G-C pairs) are relatively more stable and difficult to be invaded by ASOs (Figure 3A). This was also supported by the observation that ASO6, which shares the same sequence with ASO5 except 5 nt shorter than ASO5 at its 3′ end (Figure 3A; Table S1), was largely incapable of binding to *AZIN1* duplex (Figure 3B). In addition, DSP1 and DSP2 were only able to abolish *AZIN1* editing at 10 μM, and their editing inhibitory effects were dramatically attenuated at 200 nM (Figure S3C), suggesting that PNA-dsRNA triplex formation may not be as effective as the conventional Watson-Crick base pairing for editing inhibition. All these data suggested that ASO1, which targets the 5′ flanking region of the editing site, and the ECS-targeting ASO3 could bind to *AZIN1* and substantially inhibit (or abolish) *AZIN1* editing *in vitro*, at nanomolar concentrations.

ECS-targeting ASOs dramatically inhibit *AZIN1* editing in cancer cells

Currently, the most widely used chemistries for pre-mRNA binding and splicing modulation are the PS backbone with 2′-*O*-Me/2′-*O*-MOE/LNA or PMO, fully modified over the entire oligo length. Their stability, nuclease resistance, target affinity, and inability to trigger RNase H/RNAi response make them the ideal tools for pre-mRNA binding, splicing, and probably RNA editing. We therefore fully or partially modified ASO1 and ASO3 with PS (Figure 4A; Table S1). All 3 control ASOs (ASO-ctl, ASO-ctl2, and ASO-ctl3) were partially modified with PS at either the 5′ end or the 3′ end (Figure 4A; Table S1). We screened the basal editing level of *AZIN1* among 15 cancer cell lines (9 HCC, 3 ESCC, and 3 NSCLC). *AZIN1* editing was only detected in an ESCC line, KYSE510, and a NSCLC line, H358 (Figure S5A). Unexpectedly, all 7 ASOs that target the editing region (ASO1, 1.1, 1.2, 1.3, 5, 6, and 7) led to skipping of exon 11 in KYSE510 and H358 cells (Figure 4B; Figures S5B and S5C), possibly due to the existence of splicing factor binding sites at the editing region predicted by SpliceAid 2[32] (Figure 4C). Notably, 3 ECS-targeting ASOs (ASO3.1, 3.2, and 3.3), but not the control ASOs, inhibited *AZIN1* editing, without causing major changes in the splicing and expression of AZIN1 (Figures 4D–4F). It is likely that additional PS modification in 2′-*O*-Me-modified ASO3 increases the chemical stability, resulting in improved editing inhibition efficacies of ASO3.1, 3.2, and 3.3 in cells.

To ensure that the inhibitory effects of ASO3.1 and ASO3.2 on *AZIN1* editing are indeed due to their binding to *AZIN1* transcript *in vivo*, we confirmed that ASO could enter the nucleus (Figure 4G), as pre-mRNA editing takes place in the nucleus. By performing RNA immunoprecipitation (RIP) followed by real-time quantitative PCR (qPCR) in HEK293T cells overexpressed with Flag-tagged ADAR1 (Flag-ADAR1) or Flag empty vector control (Flag-EV), we observed that the treatment of ASO3.1 or 3.2 significantly reduced the binding of ADAR1 to *AZIN1* transcripts (Figure 4H). Of note, even though the sequence and modification patterns of ASO-ctl, ASO-ctl2, and ASO-ctl3 are not identical, all of them were unable to bind to *AZIN1* and inhibit its editing (Figures 3B and 4F).

Altogether, our findings suggested that the editing region at exon 11 of *AZIN1* pre-mRNA is non-targetable, whereas ASOs targeting the ECS could specifically and effectively inhibit ADAR1's binding to *AZIN1*, leading to suppression of *AZIN1* editing in cancer cells.

ASO3.2 specifically inhibits cancer cell viability and proliferation

We next studied whether ASO3.1 and ASO3.2 specifically inhibit cancer cell viability through repressing *AZIN1* editing. To this end, in addition to KYSE510 and H358, an *AZIN1* editing null ESCC cell line, KYSE180, was also included in the study. We observed that

concentrations as indicated. (D) *In vitro* RNA editing analysis of *AZIN1* transcripts transcribed from the FE minigene, after incubation with purified ADAR1 protein and 200 nM of the indicated ASO. Left: sequencing chromatograms illustrate editing of *in vitro* transcribed *AZIN1* transcripts in the indicated samples. Percentage of editing is calculated as area of "G" peak over the total area of "A" and "G" peaks. Black arrow indicates the position of editing site. *, no editing detected. Right: data are presented in the bar chart as the mean ± SD of technical triplicates from a representative experiment of 3 independent experiments. The value shown on the top of each bar is the mean value. n.d., not detectable.

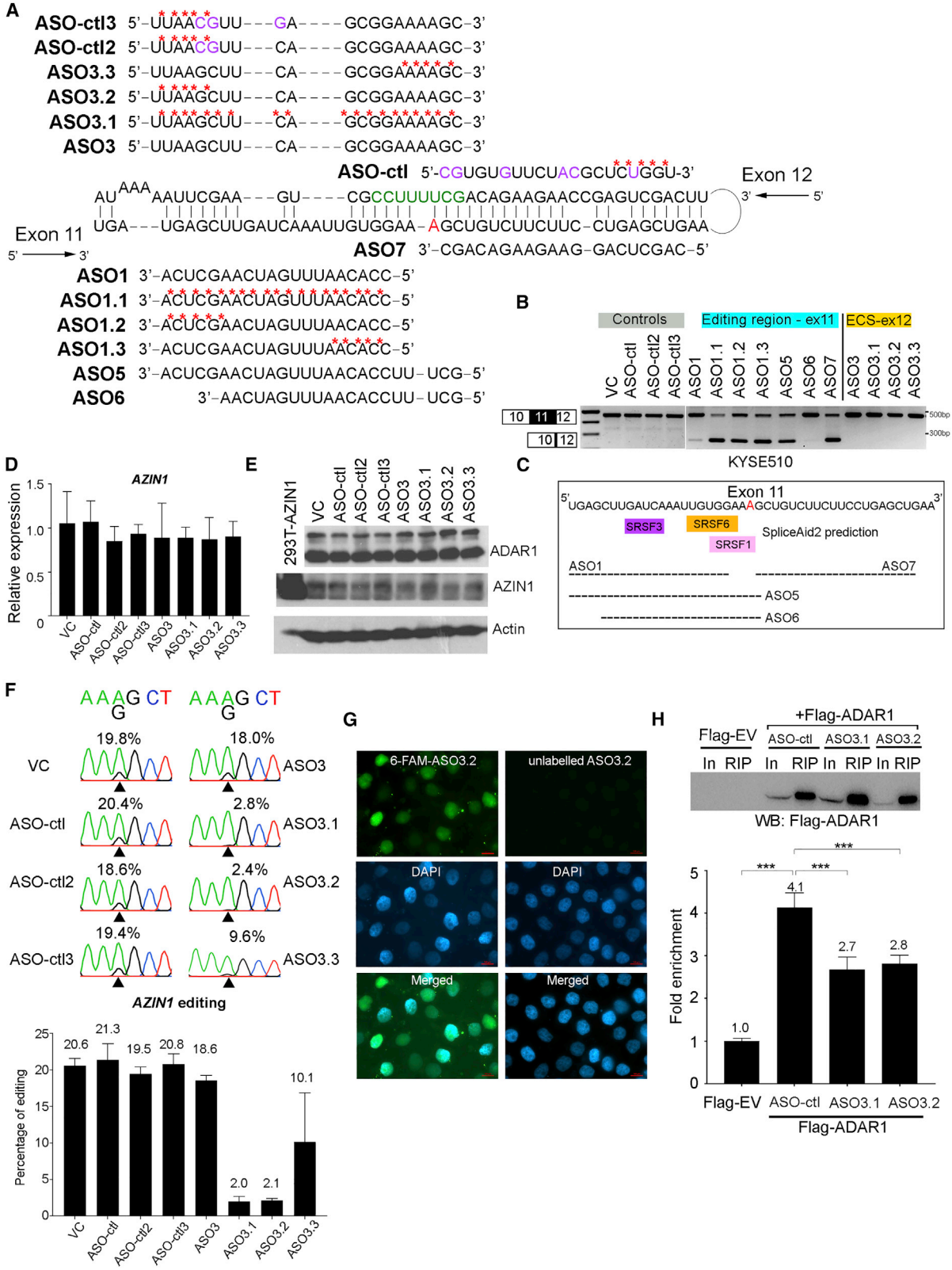

(legend on next page)

both ASO3.1 and ASO3.2 inhibited cell viability of KYSE510 and H358 with low half-maximal inhibitory concentration (IC_{50}) values (ASO3.1: K510 45.8 nM and H358 37.6 nM; ASO3.2: K510 62.3 nM and H358 48.4 nM), whereas they demonstrated much less effect on cell viability of KYSE180 (ASO3.1: 272 nM; ASO3.2: 723 nM) (Figure 5A). Of note, KYSE180 demonstrated ~2.6-fold lower sensitivity to ASO3.2 than ASO3.1, implying that ASO3.2 may confer a higher specificity to repress editing and cancer cell viability than ASO3.1 (Figure 5A). After confirming that there was no obvious difference in the effect on cancer cell viability among ASO-ctl, ASO-ctl2, and ASO-ctl3 (Figure S6), we chose ASO-ctl as the control ASO for the following experiments. To further confirm the specific inhibitory effect of ASO3.2, 3 cell lines were used for cell viability and foci formation assays. We found that ASO3.2 only inhibited cell viability of KYSE510 and H358, but not KYSE180 (Figures 5B and 5C). In addition to cancer cells, we also did not observe any obvious effect on the viability of healthy human hepatocytes, which are free of *AZIN1* editing (Figure 5B; Figure S5A).

As reported by us previously, $AZIN1^{S367G}$ could enhance G1/S transition and increase the protein expression of oncoproteins ODC and CCND1.[5] Cell cycle analysis showed that upon treatment with ASO3.2, KYSE510 and H358 cells, but not KYSE180 cells, demonstrated an increase in the percentage of sub-G1 phase (apoptotic cells). Because ~20% of ASO3.2-treated KYSE510 and H358 cells entered apoptosis from G1 or other phase of the cell cycle, we did not observe a clear attenuation of G1/S transition compared to cells treated with ASO-ctl or ASO3 (Figures 5D and 5E). However, a reduction in CCND1 and ODC protein expression was detected in ASO3.2-treated KYSE510 but not KYSE180 cells (Figure S7), suggesting that ASO3.2 could specifically inhibit *AZIN1* editing in cancer cells, leading to reduced cell viability and proliferation.

ASO3.2 effectively inhibits tumor incidence and growth *in vivo*

We next investigated the effect of ASO3.2 on tumor incidence and growth. KYSE510 cells were pre-treated with ASO-ctl or ASO3.2, followed by subcutaneous injection into dorsal flanks of mice. Tumor incidence rate of mice injected with ASO3.2-pre-treated cells was lower than the control group (Figure 6A), and tumors derived from ASO-ctl-pre-treated cells grew significantly faster than tumors originated from ASO3.2-pre-treated cells (Figure 6B). Suppression of *AZIN1* editing was also confirmed in xenograft tumors derived from ASO3.2-pre-treated cells at end point (Figure 6C).

We further investigated the impact of ASO3.2 on tumor growth by intratumoral injection. Extracellular vesicles (EVs) are small membrane vesicles released from different types of cells and increasingly being recognized as natural RNA carriers and novel drug delivery vehicles.[33,34] In this study, ASO3.2 or ASO-ctl was loaded into EVs derived from human red blood cells (RBCs) (ASO-RBCEVs), an ideal source of EVs with promising properties for RNA drug delivery.[35] To test the cellular uptake of ASO-RBCEVs, Cy5-labeled ASO3.2 was loaded into RBCEVs that were labeled with carboxyfluorescein succinimidyl ester (CFSE), which fluoresces only in the presence of esterase when they are either loaded into RBCEVs or internalized into cells.[36] Upon treatment with Cy5-ASO loaded into CFSE-RBCEVs, 100% of KYSE510 cells were Cy5 and CFSE double positive, indicating a very high cellular uptake of ASO-RBCEVs (Figure 6D). Next, mice were injected with untreated KYSE510 cells subcutaneously for tumor development, followed by administration of ASO-RBCEVs or naked (unloaded) ASO intratumorally every 4 days (Figure 6E). Notably, intratumoral injection of ASO3.2-RBCEVs significantly inhibited tumor growth, whereas no obvious difference was observed in tumor growth between mice treated with naked ASO-ctl and ASO3.2 (Figure 6F). Altogether, ASO3.2 could effectively inhibit tumor incidence and growth *in vivo*.

ASO3.2 specifically inhibits cell viability of cells derived from HCC patient-derived xenografts

To evaluate whether ASO3.2 could be a promising RNA therapeutics for cancer treatment, we went on to examine the effect of ASO3.2 on HCC PDX-derived cells. We examined the editing level of *AZIN1* in several PDX cells and identified PDX1 and PDX11 as *AZIN1* editing-positive and -negative PDX lines, respectively (Figure 6G). As seen in

Figure 4. ECS-targeting ASOs abolish or substantially inhibit *AZIN1* editing in cancer cells

(A) Illustration of chemical modifications of ASOs. 2′-*O*-Me-modified ASO1, ASO3, and control ASOs (ASO-ctl, ASO-ctl2, and ASO-ctl3) were modified with PS bonds, indicated with red asterisks (see also Table S1). Point mutations introduced into each control ASO are highlighted in purple. (B) Semiquantitative PCR analysis of *AZIN1* transcripts in KYSE510 cells that were treated with each of the indicated ASOs (100 nM) by Lipofectamine transfection. Agarose gel electrophoresis of PCR amplicons showing two isoforms of *AZIN1*. The fast-moving band indicates an exon 11-skipping isoform. Sanger sequencing chromatogram data showing the junction between exon 10 and exon 12 can be seen in Figure S5C. (C) *In silico* prediction of splicing factor binding sites on the editing region of *AZIN1* pre-mRNA by SpliceAid2.[32] SRSF3, SRSF6, and SRSF1 are predicted to bind to the editing region. Editing site is highlighted in red. (D) qPCR analysis of *AZIN1* expression in KYSE510 cells treated with 100 nM of each of the indicated ASOs by Lipofectamine transfection. Data are presented as the mean ± SD of triplicates from a representative experiment of 2 independent assays. (E) Western blot analysis of AZIN1 and ADAR1 protein expression in the same cells described in (D). Approximately 5 μg of protein lysate extracted from HEK293T cells transfected with *AZIN1* expression construct was included as a positive control for AZIN1 protein. β-Actin (Actin) was used as a loading control. (F) Sequencing chromatograms show editing of *AZIN1* transcripts in the same cells described in (D). Percentage of editing is calculated as area of "G" peak over the total area of "A" and "G" peaks. Data are presented in the bar chart as the mean ± SD of technical triplicates from a representative experiment of 3 independent experiments. The value shown on the top of each bar is the mean value. (G) Representative fluorescence microscopy images of KYSE510 cells treated with 100 nM unlabeled or 6-FAM-labeled ASO3.2. DAPI staining (blue) indicates the nuclei. Scale bar, 500 μm. (H) RIP-qPCR analysis of the binding of ADAR1 protein to *AZIN1* transcripts in HEK293T cells that were overexpressed with Flag-tagged ADAR1 (Flag-ADAR1) or Flag empty vector (Flag-EV), under no treatment or treatment with the indicated ASO. The Western blot (using anti-Flag antibody) and qPCR analyses of Flag-RIP immunoprecipitates are shown at top and bottom, respectively. Data are presented as mean ± SD of technical triplicates. Input (In) indicates 1% of the total cell lysate. Statistical significance is determined by unpaired, two-tailed Student's t test (***$p < 0.001$).

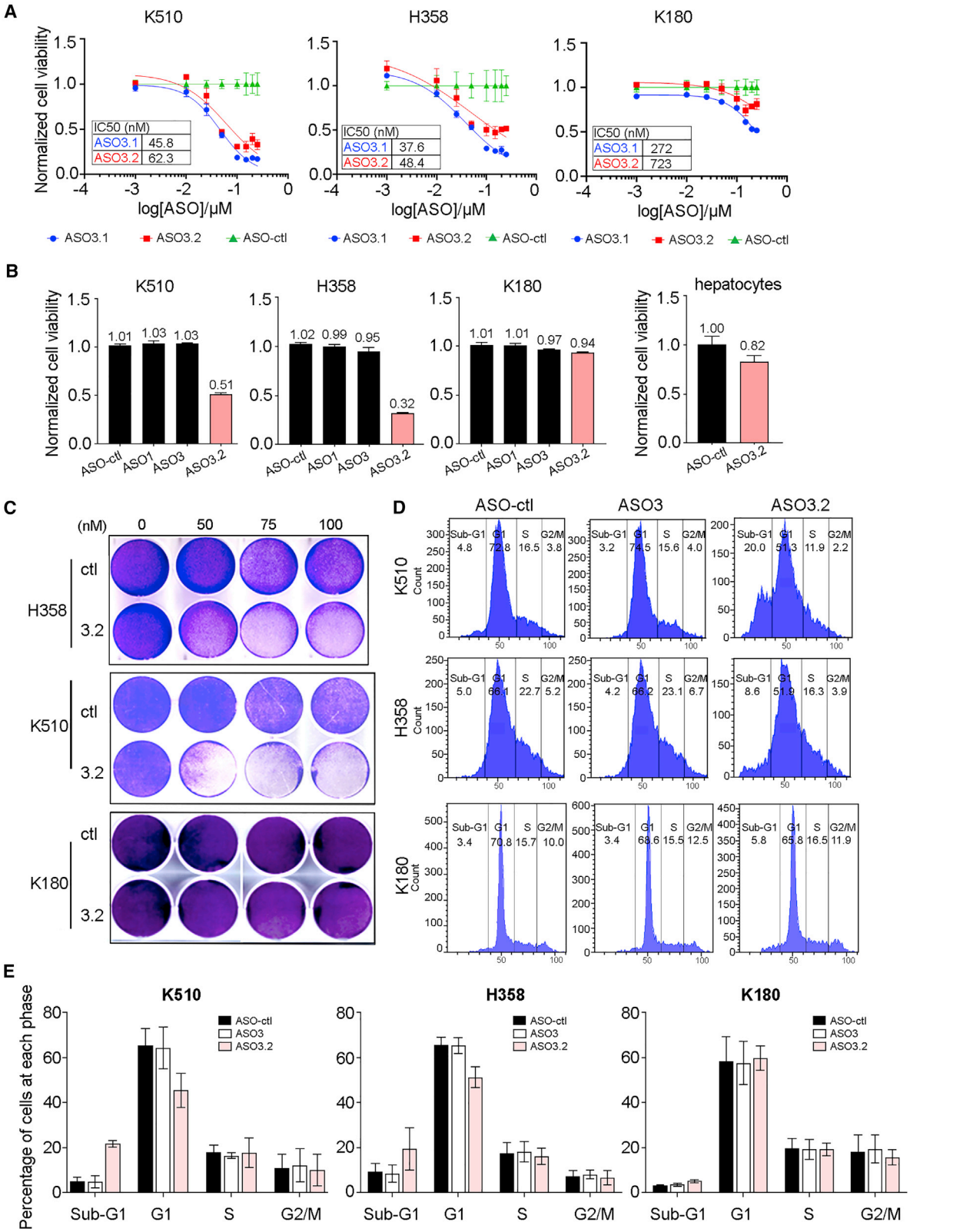

(legend on next page)

Figure 6H, PDX1 demonstrated significantly reduced cell viability upon ASO3.2 treatment, whereas no obvious changes in cell viability were observed in PDX11 cells.

DISCUSSION

As reported by us and others in the past decade, dysregulated A-to-I editing is implicated in the pathogenesis of various cancers, such as breast cancer,[37] glioma,[16,38] multiple myeloma (MM),[7] chronic myeloid leukemia,[39] HCC,[3,19] CRC,[5] gastric cancer,[40] and ESCC.[4,41] Transcripts aberrantly edited by ADARs in cancer tissues such as *AZIN1*,[3] *GLI1*[7] (glioma-associated oncogene 1), and *DHFR*[42] (dihydrofolate reductase) remarkably contribute to cancer progression and metastasis. Unlike DNA editing, genetic information manipulated by RNA editing is reversible and tunable. Since ADAR1 has multiple functions that are critical for normal development such as hematopoiesis and organ development,[43] simply modulating the expression of ADARs may cause considerable off-target effects. An alternative strategy may be to disrupt ADAR enzymes to specific editing sites at target transcripts.

We were the first to report that ADAR1-mediated editing at codon 367 of AZIN1 produces a much more aggressive form, AZIN1^{S367G}, than the wild-type AZIN1, and the increased level of AZIN1^{S367G} predisposes to HCC[3] and ESCC.[4] Later on, several groups reported that increased *AZIN1* editing is implicated in other types of cancer such as NSCLC[6] and CRC.[5] All these findings suggest that targeting *AZIN1* editing holds great promise for cancer treatment. To achieve the goal of repressing cancer-associated *AZIN1* editing in cells and tissues, ASOs were chosen, due to the facts that (1) they are smallest (~15–25-mer) among all RNA-based therapeutics; (2) they have high ability to enter cells through liposome formulation or conjugation with cell-penetrating moieties; and (3) they can be modified to have adequate stability and target binding affinity as well as less immunogenicity.

Like splice-switching and translation-inhibiting ASOs, these editing-inhibiting ASOs must bind to target pre-mRNA transcripts in the nucleus, without eliciting RNase H activation or RNAi. The 2′-*O*-methyl group that substitutes the hydrogen at the 2′ of RNA (2′-*O*-Me-RNA) exists in physiological conditions. This modification increases both nuclease resistance and target binding affinity (by 0.9°C/modification), while it decreases native immune reactions.[44] To target A-to-I RNA editing, it is very important to identify the ECS and understand the secondary structure of the target RNA (i.e., which nucleotide is in a base pair, hairpin loop, or bulge). This information will be very helpful to designing ASOs targeting either the editing region or the ECS, without disturbing the potential binding of RNA-binding proteins (RBPs) (e.g., splicing factors). In addition, a properly designed ASO-based editing inhibitor is expected to invade the secondary structure to prevent editing.[26] In this study, we uncover that the 3′ end sequence of *AZIN1* exon 12 forms dsRNA with the editing region, allowing us to design and synthesize multiple 2′-*O*-Me/PS-modified ASOs and PNAs that target either the editing region or the ECS. We observed that (1) ASO1 or ASO3 could either substantially inhibit or completely abolish *AZIN1* editing *in vitro*, respectively, (2) ASO2, 4, and 6 were incapable of binding to *AZIN1* duplex, and (3) although ASO7 could bind to *AZIN1*, it still failed to inhibit editing *in vitro*. All these observations suggest that the 5′ upstream sequence of the editing site and the 3′ downstream sequence of the ECS may favor the binding of ASO to *AZIN1* and the consequent inhibition of ADAR1 binding. This information may be useful for future understanding of ADAR1 substrate binding and deamination. However, whether ASO1 and ASO3 inhibit *AZIN1* editing by a strand-invasion mechanism remains for our investigation.

Moreover, it has been reported that PNAs incorporating modified nucleobase such as thio-pseudoisocytosine (L) and guanidine-modified 5-methyl cytosine (Q) can selectively bind to dsRNAs over single-stranded RNAs and dsDNAs in a sequence-specific manner.[45–49] Besides, PNAs have a neutral peptide-like backbone, are chemically stable and resistant to nucleases, and offer enhanced specificity of RNA sequence and structure recognition.[46,50,51] In this study, we also tested the inhibitory effect of PNAs on *AZIN1* editing. As ASO4 (20-mer) was unable to bind to *AZIN1* duplex, it is not surprising that the antisense PNA ASP1 (12-mer) was also incapable of binding to *AZIN1*. Although dsRNA-binding PNAs DSP1 and DSP2 could bind to *AZIN1* with modest affinity, they failed to inhibit editing at nanomolar concentrations, possibly attributed to the insufficient blockage of ADAR1-*AZIN1* dsRNA interaction by DSP1 (10-mer) or DSP2 (8-mer) due to their rather short length. All these observations imply that a relatively long and chemically stable ASO (e.g., complete 2′-*O*-Me sugar ring modification in combination with partial PS backbone modification) may be an optimal chemistry for RNA editing inhibition. However, it is interesting to test whether additional modifications (e.g., LNA) of 2′-*O*-Me or 2′-*O*-Me/PS-modified ASOs would further improve the editing inhibitory potency *in vitro* and *in vivo*.

Although ASO1 demonstrates promising editing inhibitory effect *in vitro*, we found that ASO1 and other ASOs that target the 43-nt

Figure 5. ASO3.2 specifically inhibits cancer cell viability and proliferation

(A) Cell viability of KYSE510 (K510), H358, or KYSE180 (K180) cells was measured by CellTiter-Glo (CTG) assays, after treatment with the indicated concentrations of ASO3.1, ASO 3.2, or ASO-ctl by Lipofectamine transfection for 48 h. The corresponding IC_{50} values are shown for each cell line. Data are presented as the mean ± SD of 4 replicates from a representative experiment of 3 independent assays. (B) Cell viability of each cancer cell line or normal hepatocytes isolated from the perfused livers of humanized mice was measured by CTG assays after treatment with 50 nM ASO3.2 or ASO-ctl for 48 h. ASO1 and ASO3 serve as 2 additional negative controls, because of their incapability of inhibiting *AZIN1* editing. (C) Foci formation assay of each of 3 cell lines after being treated with ASO3.2 or ASO-ctl at the indicated concentrations for 48 h. Cells were stained with crystal violet. (D and E) Representative cell cycle analysis by flow cytometry. Cells were treated with 50 nM ASO3, ASO3.2, or ASO-ctl for 48 h, followed by PI staining and cell cycle analysis. The original FACS data were analyzed with BD FACSDiva Software, which plots the cell count versus DNA content. The value indicates the percentage of the indicated cells at sub-G1, G1, S, or G2/M phase. Data are presented as the mean ± SD of 3 biological triplicates in the bar charts (E).

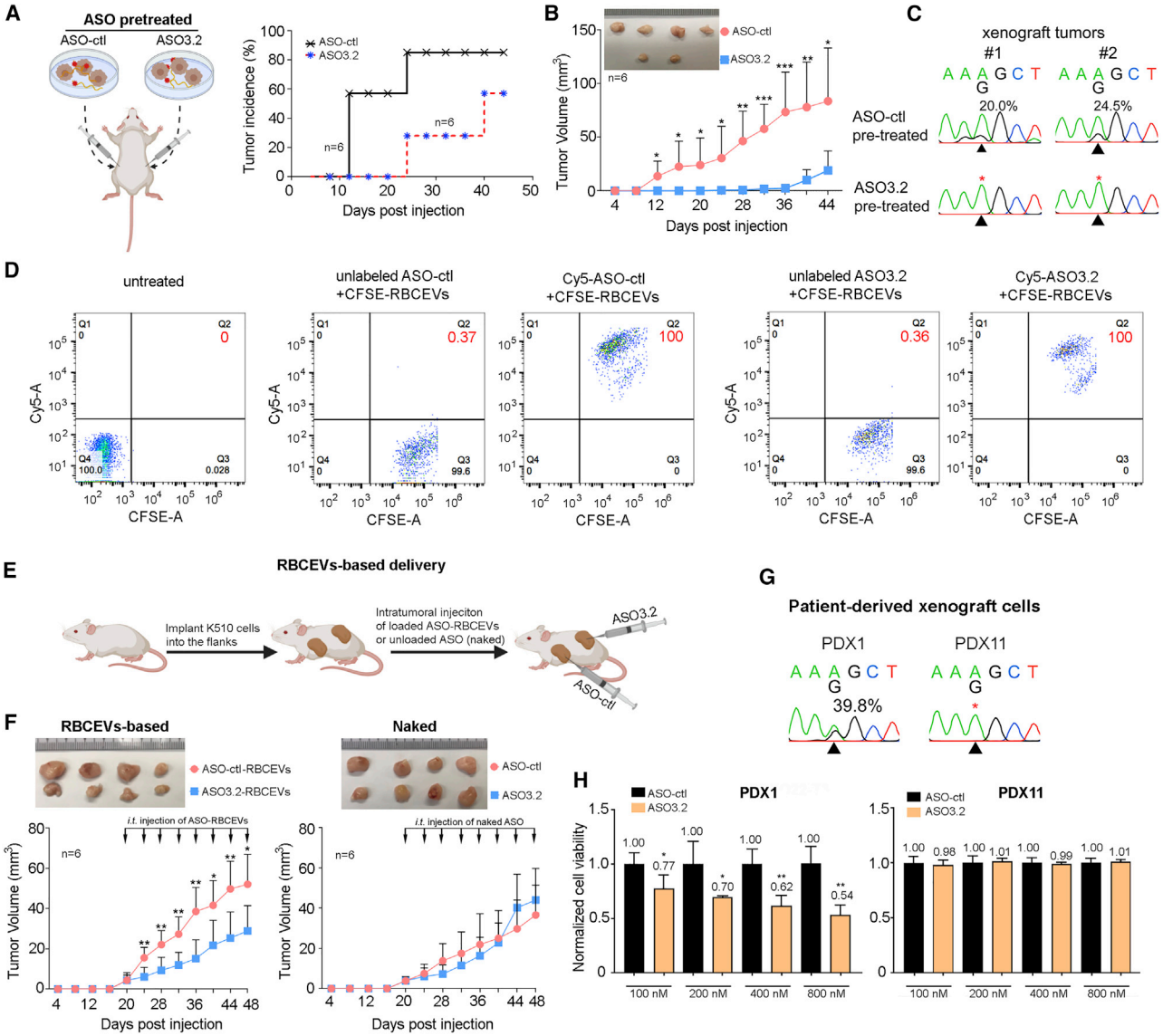

Figure 6. ASO3.2 specifically inhibits tumor incidence and growth *in vivo*

(A) Left: schema of subcutaneous injection of ASO-pretreated KYSE510 cells into mice. ASO3.2- or ASO-ctl-pre-treated cells were injected into right or left dorsal flank of mice, respectively. Right: cumulative tumor incidence curves of mice injected with the indicated pre-treated cells (100 nM ASO3.2 or ASO-ctl for 48 h), estimated by the Kaplan-Meier method. (B) Representative tumors derived from pre-treated KYSE510 cells as described above 6 weeks after subcutaneous injection (n = 6 mice per group). Growth curves of tumors derived from the indicated cells over a period of 6 weeks. Data are presented as the mean ± SD. (C) Sequencing chromatograms illustrate editing of *AZIN1* in 2 representative pairs of xenograft tumors. (D) FACS analysis of Cy5 versus CFSE fluorescence in KYSE510 cells treated with 50 nM unlabeled or Cy5-labeled ASO-ctl/ASO3.2 that were loaded into the CFSE-labeled RBCEVs. Percentages of Cy5/CFSE double-positive cells (Q2) are highlighted in red. (E) Schema of RBCEV-based ASO delivery to mice bearing cancer xenografts. (F) Left: representative tumors derived from KYSE510 cells after receiving i.t. injection of ASO3.2-RBCEVs or ASO-ctl-RBCEVs every 4 days (n = 6 mice per group). For each injection, a total of 1 μg of ASO was loaded into 50 μg of RBCEVs and resuspended in 20 μL of PBS. Right: representative tumors after receiving multiple i.t. injections of naked (unloaded) ASO3.2 or ASO-ctl. The same experimental procedures were conducted as described on left. Growth curves of each group of tumors over a period of 7 weeks. Data are presented as the mean ± SD. Black arrow indicates each injection. (G) Sequencing chromatograms illustrate editing of *AZIN1* in PDX1 and PDX11 cells. (H) Cell viability of PDX1 or PDX11 cells was measured by CTG assays after treatment with ASO3.2 or ASO-ctl by Lipofectamine transfection for 48 h. Data are presented as the mean ± SD of 4 replicates from a representative experiment of 2 independent experiments. (B, F, and H) *$p < 0.05$, **$p < 0.01$, ***$p < 0.001$ determined by unpaired, two-tailed Student's t test.

editing region led to a substantial exon 11 skipping, probably due to the blockage of splicing regulators (e.g., SRSF1, SRSF3, SRSF6) to the editing region, suggesting that the editing region is not targetable. Moreover, even though 2′-*O*-Me-modified ASO3 that targets the ECS could completely abolish *AZIN1* editing *in vitro*, only ASO3.1 and ASO3.2, which have further complete and partial PS modification respectively, could effectively abolish *AZIN1* editing in cancer cells. This could be due to the advantages of PS modification such as strong resistance to endo- and exonuclease digestion, increased serum stability, and reduced renal clearance. It is also known that PS modification may cause non-specific binding to plasma proteins and other nucleotide sequences. This may explain why the fully PS-modified ASO3.1 demonstrated less specificity of inhibition of *AZIN1* editing and tumor cell viability than the partially PS-modified ASO3.2. We further confirmed that ASO3.2 specifically inhibited cell viability of $AZIN1^{S367G}$-expressing cancer cells and cells derived from HCC PDXs but not $AZIN1^{S367G}$-null cancer cells, PDX lines, and normal hepatocytes. Further, in the pre-treated xenograft tumor model, ASO3.2 inhibited tumor incidence and growth. This observation was also supported by the intratumoral injection model in which we delivered ASO3.2 into tumor cells with an RBCEV-based delivery approach and found that intratumoral injection of ASO3.2 that was loaded into RBCEVs, but not naked (unloaded) ASO3.2, significantly suppressed tumor growth.

Until now, 4 ASOs have been clinically approved, all of which are chemically modified. Two recently FDA-approved splicing-switch ASOs, eteplirsen and nusinersen, entered the clinic in 2016/2017, raising the enthusiasm in the field for developing ASO therapeutics for treating diseases. In this study, we show that ASO-mediated inhibition of *AZIN1* editing effectively suppresses tumor incidence and growth, suggesting that many cancer patients, particularly those demonstrating high editing level of *AZIN1* in tumors, may benefit from this *AZIN1*-targeting, ASO-based therapeutics.

MATERIALS AND METHODS

Cell lines

All cell lines were maintained in RPMI-1640 medium (Biowest) supplemented with 10% fetal bovine serum (FBS) (Biowest). All cell lines used in this study were regularly authenticated by morphological observation and tested for mycoplasma contamination. PDX lines were cultured in DMEM-F12 (Biowest) and supplemented with 1:50 B27 supplement without vitamin A (Thermo Fisher), 1:100 insulin-transferrin-selenium supplement (Gibco), 1.25 mM *N*-acetyl-L-cysteine (Sigma-Aldrich), 10 mM nicotinamide (Sigma-Aldrich), 10 nM recombinant human (Leu15)-gastrin I (Sigma-Aldrich), 25 ng/mL recombinant human hepatocyte growth factor (HGF) (Abcam), 50 ng/mL recombinant human epidermal growth factor (EGF) (Abcam), 50 ng/mL recombinant human basic fibroblast growth factor (bFGF) (Abcam), 5 μg/mL heparin (Sigma-Aldrich), and 10 ng/mL recombinant human FGF-10 (Abcam). All cancer cell lines and PDX lines were incubated at 37°C in a humidified incubator containing 5% CO_2.

Normal human hepatocytes

HepaCur human hepatocytes are isolated from the perfused livers of humanized FRG KO mice. The freshly isolated hepatocytes are guaranteed to be ≥95% human and have a viability of ≥70%. Isolated hepatocytes were cultured in HypoThermosol FRS (BioLife Solutions, catalog # 101373), which is an optimized hypothermic preservation medium. Prior to plating, HypoThermosol FRS was changed to HMM (HepaCur Maintenance Medium, catalog # HMM500), according to the manufacturer's protocol. Subsequently, 1×10^4 cells were plated into each well of a 96-well plate and treated with ASOs on the same day. The cells were incubated at 37°C in a humidified incubator containing 5% CO_2.

RNA extraction, cDNA synthesis, quantitative PCR, and Sanger sequencing

Total RNA was extracted with the RNeasy Mini Kit (QIAGEN), according to the manufacturer's protocol. cDNA synthesis was conducted with the Advantage Reverse Transcription Kit (Clontech Laboratories), following the manufacturer's protocol. Real-time qPCR was performed with GoTaq DNA polymerase (Promega) on the QuantStudio 5 Real-Time PCR System (Applied Biosystems). The relative expression of *AZIN1* or *ADAR1* (defined as "relative expression") is given as $2^{-\Delta CT}$ ($\Delta C_T = C_T(AZIN1/ADAR1) - C_T(\beta\text{-actin})$) and normalized to the relative expression that was detected in the corresponding control cells, which was defined as 1.0. Semiquantitative PCR was done with the FastStart Taq Kit (Roche), following the manufacturer's protocol. Purified PCR amplicons were identified by Sanger sequencing. ImageJ was used to calculate the percentage of A-to-I(G) editing. The percentage of editing is calculated as the area of "G" peak over the total area of "A" and "G" peaks. Sequences of primers are listed in Table S2.

Generation of minigene constructs

To clone *AZIN1* sequences for the pRK7 or pcDNA3.1 minigene construction, placental DNA (Sigma-Aldrich) was used for PCR using PrimeSTAR Max DNA Polymerase (Takara), following the manufacturer's protocol. The KAPA HiFi HotStart PCR Kit (KAPA Biosystems) was utilized to introduce internal deletion or point mutations. Sequences of primers used for cloning are listed in Table S2.

In vitro RNA editing assay

First, forced overexpression of Flag-tagged ADAR1 protein was performed by transfecting Flag-ADAR1 plasmid into HEK293T cells. Cells were harvested 48 h after transfection and lysed in lysis buffer containing 50 mM Tris-HCl pH 7.5 (Ambion), 150 mM NaCl (Ambion), 1 mM EDTA (Ambion), Triton X-100 (Sigma-Aldrich), and 1× cOmplete EDTA-free Protease Inhibitor Cocktail (Roche). Anti-FLAG M2 Magnetic Beads (Sigma-Aldrich) were used for immunoprecipitation of cell lysate to obtain Flag-ADAR1 proteins. 100 μg/mL Flag elution buffer was obtained by dissolving 3× FLAG peptide (Sigma) in Tris-buffered saline (TBS) containing 50 mM Tris-HCl pH 7.4 and 150 mM NaCl. Flag elution buffer was used to elute the proteins from the magnetic beads. Eluant was stored at −80°C until further use. *In vitro* transcription of the minigene constructs was done with the RiboMAX Large Scale RNA Production System-SP6

(Promega), following the manufacturer's protocol. Next, incubation of 5 μL of Flag-ADAR1 protein and purified RNA transcripts that were transcribed from the *AZIN1* FE minigene was carried out at 37°C for 3 h, followed by RNA cleaning-up using the RNeasy Mini Kit (QIAGEN) and cDNA synthesis.

To test the editing inhibitory effect of ASOs *in vitro*, ASOs were incubated with *in vitro* transcribed RNA transcripts prior to the addition of purified ADAR1 protein. PCR amplification was then conducted, and purified PCR products were sent for Sanger sequencing. Sequences of primers used for *in vitro* editing analysis are listed in Table S2.

RNA electrophoretic mobility shift assay

Binding of each oligo to the AZIN1 RNA duplex probe

The 86-nt *AZIN1* RNA duplex probe was transcribed *in vitro* with RiboMAX Large Scale RNA Production System-T7 (Promega), following the manufacturer's protocol. Next, 50 pmol of the RNA probe was incubated at 37°C for 30 min with rSAP (shrimp alkaline phosphatase) (NEB) to dephosphorylate the RNA. EDTA (0.8 μL, 250 mM) was added and incubated at 65°C for 20 min to heat inactivate rSAP. The mixture was then incubated with 1 μL of 100 mM $MgCl_2$ with T4 PNK (polynucleotide kinase) (NEB) and ATP, [γ-^{32}P] (PerkinElmer) at 37°C for 30 min. The mixture was then heated to 95°C to denature the duplex and was left to anneal slowly to room temperature, after which 80 μL of distilled water was added and transferred to an Illustra MicroSpin G-25 Column (GE Healthcare) for purification. LightShift Chemiluminescent RNA EMSA Kit (Thermo Scientific) 10× REMSA Binding Buffer (100 mM HEPES pH 7.3, 200 mM KCl, 10 mM $MgCl_2$, 10 mM DTT) was used to incubate the samples. Samples were mixed with 1 μL of RNA duplex (with a final concentration of 25 nM) and the respective oligonucleotides and incubated for 30 min. TBE (Tris-borate EDTA) gel was pre-run before samples were added. The gel was dried and then exposed to BioMax Light Film (Carestream, Sigma-Aldrich) and developed.

Binding of each PNA to the truncated AZIN1 RNA duplex probe

Both strands (ECS-s and ES-s) were added together and slowly cooled from 95°C to room temperature to form the truncated RNA duplex before annealing of the PNAs at 40°C for 10 min. Both steps were carried out in an incubation buffer of 200 mM NaCl, 0.5 mM EDTA, and 20 mM HEPES, pH 7.5. After annealing of the PNA, the samples were allowed to cool to room temperature before incubation at 4°C overnight. The gel was run at constant voltage of 250 V for 5 h in a running buffer of 1× TBE, pH 8.3. The gel was then stained in ethidium bromide for 30 min before it was imaged with the Typhoon Trio Variable Mode Imager.

Sequences of probes are listed in Table S3.

ASO treatment

All ASOs were purchased from Integrated DNA Technologies (IDT). PNAs (ASP1 and DSP1 and DSP2) were synthesized and purified according to the protocol reported previously.[49] Cells were seeded the day before treatment to achieve 50% confluency on the day of treatment. Cells were then treated (transfected) with ASOs that were diluted in Opti-MEM to the desired concentration by Lipofectamine 2000. The subsequent analysis was conducted 48 h after the treatment with ASO. Three independent experiments were carried out, each with three technical replicates conducted.

RNA immunoprecipitation

HEK293 cells were either untreated or treated with ASO-ctl or ASO3.2 for 6 h, followed by transfection with 4 μg of Flag empty vector (Flag-EV) or Flag-tagged ADAR1 (Flag-ADAR1). At 48 h after transfection, cells were collected and lysed in buffer containing 50 mM Tris, pH 7.5, 150 mM NaCl, 1 mM EDTA, and 1% Triton X-100 supplemented with cOmplete protease inhibitor (Roche) and SUPERase In (Invitrogen). Lysate was then incubated with anti-FLAG M2 magnetic beads (Sigma) overnight at 4°C with rotation, followed by of washing 6 times with 1× TBS buffer (50 mM Tris and 150 mM NaCl). A total of 10% of beads was used for protein elution, and the rest was used for RNA extraction using the RNeasy miniprep kit (QIAGEN). Extracted RNA was reverse transcribed with the Advantage RT-for-PCR Kit (Clontech) with oligo dT, and subsequently qPCR was performed. %Input = $2^{-\Delta Ct} \times 100$; $\Delta Ct = Ct_{RIP} - [Ct_{input} - \text{dilution factor}]$. Fold enrichment was calculated by normalizing the "%Input (each sample)" to "%Input (Flag-EV)."

Cell viability assay

The CellTiter-Glo Luminescent Cell Viability (CTG) Assay (Promega) was used to measure cell viability after cells were treated with ASOs. Cells were seeded and treated in 96-well clear flat-bottom plates (Corning) for 2 days prior to the addition of the CTG assay reagent. A total of 100 μL of cell lysate was transferred to a 96-well white flat-bottom plate (Corning). The GloMax Discover Microplate Reader (Promega) was used to read the intensity of luminescence.

Western blot analysis

Protein lysates were prepared with Radioimmunoprecipitation assay (RIPA) buffer (Sigma) supplemented with 1× cOmplete EDTA-free Protease Inhibitor Cocktail (Roche) and quantified by Bradford assay (Bio-Rad). Protein lysates were then separated by 8%–10% SDS-PAGE, followed by incubation with primary antibodies (1:1,000 dilution) overnight at 4°C and incubation with secondary antibodies (1:10,000 dilution) at room temperature for 1 h. Primary antibodies used are anti-ADAR1 (Abcam, ab88574), anti-AZIN1 (Proteintech, 11548-1-AP), anti-β-actin (1:10,000; Santa Cruz Biotechnology, sc-47778), anti-Flag-horseradish peroxidase (1:10,000; Sigma-Aldrich, A8592), anti-ODC (Proteintech, 28728-1-AP), and anti-CCND1 (Proteintech, 60186-1-Ig).

Foci formation assay

For foci formation assay, cells were seeded to obtain 50% confluency prior to the treatment of ASO. Cells were stained with crystal violet (Sigma-Aldrich) 48 h after treatment.

Cell cycle analysis by PI staining and fluorescence-activated cell sorting

Cells were treated with ASOs for 48 h prior to the cell cycle analysis. After the treatment, cells were fixed with 70% ethanol in −20°C overnight. After washing with phosphate-buffered saline (PBS; 10 mM phosphate, 137 mM NaCl, and 2.7 mM KCl), cells were resuspended in 1 mL of staining solution containing 50 μg/mL propidium iodide (PI) (Invitrogen) and 0.5 μL of 10 mg/mL RNase (Thermo Scientific) and incubated for 1 h at 37°C. Stained cells were analyzed on the LSRII (BD Biosciences), and the results were analyzed on FACSDiva Software (BD Biosciences).

Loading of ASO into RBCEVs

Blood samples were obtained from healthy donors by Hong Kong Red Cross, and EVs were produced from RBCs according to our established protocol.[35] ASOs were loaded into RBCEVs at a ratio of 1 to 50 with ExoFect Transfection Reagent (System Biosciences) according to the manufacturer's protocol. RBCEVs were washed twice with PBS at 21,000 × *g* for 30 min at 4°C to remove the free ASOs and transfection reagent.

Labeling RBCEVs with CFSE

A total of 200 μg of ASO-loaded RBCEVs was incubated with 400 μL of 10 μM CFSE at 37°C for 2 h. A total of 0.5 mL of CFSE-labeled RBCEVs was loaded onto a prepacked qEV-original size exclusion column (Izon Science, Christchurch, New Zealand) and eluted with PBS in 40 fractions (0.5 mL/fraction). Fractions 7 to 11 were combined and centrifuged at 21,000 × *g* for 30 min at 4°C. The supernatant was removed, and the RBCEV pellet was washed twice with PBS, resuspended, and quantified with a NanoDrop spectrophotometer (Thermo Fisher).

Fluorescence imaging

Cells were cultured on coverslips for 24 h and treated with 100 nM unlabeled or 6-carboxyfluorescein (6-FAM)-labeled ASO3.2. At 48 h after treatment, cells were washed with PBS before fixation with methanol for 10 min at room temperature. Fixed cells were washed with PBS thrice for 5 min each. The coverslips were mounted onto slides with SlowFade Gold Antifade Mountant with DAPI (Thermo Fisher Scientific) and viewed under a Zeiss Axio Imager M2 microscope.

Cellular uptake of ASOs by flow cytometry analysis

KYSE510 cells were treated with either Cy5-labeled or unlabeled ASO-ctl/ASO3.2 that were loaded into CFSE-labeled RBCEVs (at a ratio of 1 to 50). After 48 h, cells were trypsinized, washed, and resuspended in the fluorescence-activated cell sorting (FACS) buffer (PBS containing 0.5% FBS). Flow cytometry of cells was performed with LSRII (BD Biosciences) and analyzed on FACSDiva Software (BD Biosciences). The cells were initially gated based on FSC-A and SSC-A to exclude the debris and dead cells (low FSC-A). The cells were further gated based on FSC-width versus FSC-height, to exclude doublets and aggregates. Subsequently, the CFSE-positive cells were gated in fluorescein isothiocyanate (FITC). Cy5-positive cells were gated with Cy5.

In vivo tumorigenicity assays

Pre-treatment model

KYSE510 cells were pre-treated with 100 nM ASO3.2 and ASO-ctl using Lipofectamine 2000 (Invitrogen) for 48 h, followed by the subcutaneous injection of 4×10^6 pre-treated cells into left and right dorsal flanks of 4- to 6-week-old NOD scid gamma (NSG) mice (n = 6 mice per group). Tumor growth was monitored by measuring tumor length (L) and width (W) at indicated time points. Tumor volume was calculated by the formula $V = 0.5 \times L \times W^2$. All animal experiments were approved by and performed in accordance with the Institutional Animal Care and Use Committees of National University of Singapore (NUS, Singapore).

Intratumoral injection model

A total of 2×10^6 KYSE510 cells were injected subcutaneously to the right and left flanks of 4- to 6-week-old NSG mice for tumor development. When tumors were visible (~1 mm in diameter), mice were divided into two groups (6 mice per group) for multiple intratumoral (i.t.) injection of ASO-loaded RBCEVs (Group 1: RBCEVs-based delivery) or naked ASO (Group 2: naked ASO) every 4 days for 7 weeks. For each injection of ASO-loaded RBCEVs per tumor, a total of 1 μg of ASO was loaded into 50 μg of RBCEVs and resuspended in 20 μL of PBS. For each injection of naked ASO per tumor, a total of 13.5 μg of ASOs (ASO-ctl or ASO3.2) was dissolved in 20 μL of PBS. Tumor growth was monitored by measuring tumor length (L) and width (W) at indicated time points. Tumor volume was calculated by the formula $V = 0.5 \times L \times W^2$. All animal experiments were approved by and performed in accordance with the Institutional Animal Care and Use Committees of National University of Singapore (NUS, Singapore).

Statistical analysis

Unpaired, two-tailed Student's t test was used for statistical analysis of changes in cell viability and tumor growth rate between the control and treatment groups. For all figures: *$p < 0.05$; **$p < 0.01$; ***$p < 0.001$.

SUPPLEMENTAL INFORMATION

Supplemental information can be found online at https://doi.org/10.1016/j.ymthe.2021.05.008.

ACKNOWLEDGMENTS

We thank and acknowledge Professor Tsao (Director, Faculty Core Facility, Li Ka Shing Faculty of Medicine, The University of Hong Kong) for providing KYSE510, KYSE180, and EC109 cells. We thank Professor Goh Boon Cher (Senior Principal Investigator, Cancer Science Institute of Singapore, National University of Singapore, Singapore) for providing H358 cells.

This project was supported by National Research Foundation Singapore; Singapore Ministry of Education under its Research Centres of Excellence initiative; Singapore Ministry of Education's Tier 2

Grants (MOE2018-T2-1-005, MOE2019-T2-2-008, MOE2015-T2-1-028, and MOE2019-T2-1-062); NMRC Clinician Scientist-Individual Research Grant (CS-IRG, project ID: MOH-000214); and Singapore Ministry of Education's Tier 3 Grants (MOE2014-T3-1-006). G.C. is also supported by The Chinese University of Hong Kong, Shenzhen (CUHK-Shenzhen) University Development Fund.

AUTHOR CONTRIBUTIONS

L.C. conceived and supervised the study. L.C. and D.J.T.T. designed and performed the experiments. J.H., Y.S., T.H.M.C., S.J.T., W.L.G., and H.H. assisted in conducting minigene construction, *in vitro* editing assay, REMSA, and cell cycle analysis. B.P. and M.T.N.L. helped to purify, load, and label RBCEVs. T.B.T., L.H., Y.Y.D., L.Z., G.K.B., and P.K.-H.C. helped to establish PDX models and to provide us with PDX-derived cells. D.-F.K.T., M.S.K., K.M.P., M.M., T.P.L., and G.C. assisted in design and synthesis of PNAs. T.B.T., G.C., M.T.N.L., and S.J.T. provided insightful suggestions and experimental materials. L.C. and D.J.T.T. wrote the manuscript.

DECLARATION OF INTERESTS

L.C., D.J.T.T., and G.C. are inventors in a patent application under the Patent Cooperation Treaty (PCT) (PCT/SG2020/050380) that is related to the work that is described in this manuscript. The other authors declare no competing interests.

REFERENCES

1. Nishikura, K. (2010). Functions and regulation of RNA editing by ADAR deaminases. Annu. Rev. Biochem. *79*, 321–349.
2. Keegan, L.P., Leroy, A., Sproul, D., and O'Connell, M.A. (2004). Adenosine deaminases acting on RNA (ADARs): RNA-editing enzymes. Genome Biol. *5*, 209.
3. Chen, L., Li, Y., Lin, C.H., Chan, T.H., Chow, R.K., Song, Y., Liu, M., Yuan, Y.F., Fu, L., Kong, K.L., et al. (2013). Recoding RNA editing of AZIN1 predisposes to hepatocellular carcinoma. Nat. Med. *19*, 209–216.
4. Qin, Y.R., Qiao, J.J., Chan, T.H., Zhu, Y.H., Li, F.F., Liu, H., Fei, J., Li, Y., Guan, X.Y., and Chen, L. (2014). Adenosine-to-inosine RNA editing mediated by ADARs in esophageal squamous cell carcinoma. Cancer Res. *74*, 840–851.
5. Shigeyasu, K., Okugawa, Y., Toden, S., Miyoshi, J., Toiyama, Y., Nagasaka, T., Takahashi, N., Kusunoki, M., Takayama, T., Yamada, Y., et al. (2018). AZIN1 RNA editing confers cancer stemness and enhances oncogenic potential in colorectal cancer. JCI Insight *3*, e99976.
6. Hu, X., Chen, J., Shi, X., Feng, F., Lau, K.W., Chen, Y., Chen, Y., Jiang, L., Cui, F., Zhang, Y., et al. (2017). RNA editing of AZIN1 induces the malignant progression of non-small-cell lung cancers. Tumour Biol. *39*, 1010428317700001.
7. Lazzari, E., Mondala, P.K., Santos, N.D., Miller, A.C., Pineda, G., Jiang, Q., Leu, H., Ali, S.A., Ganesan, A.P., Wu, C.N., et al. (2017). Alu-dependent RNA editing of GLI1 promotes malignant regeneration in multiple myeloma. Nat. Commun. *8*, 1922.
8. Teoh, P.J., An, O., Chung, T.H., Chooi, J.Y., Toh, S.H.M., Fan, S., Wang, W., Koh, B.T.H., Fullwood, M.J., Ooi, M.G., et al. (2018). Aberrant hyperediting of the myeloma transcriptome by ADAR1 confers oncogenicity and is a marker of poor prognosis. Blood *132*, 1304–1317.
9. Rueter, S.M., Dawson, T.R., and Emeson, R.B. (1999). Regulation of alternative splicing by RNA editing. Nature *399*, 75–80.
10. Kawahara, Y., Zinshteyn, B., Sethupathy, P., Iizasa, H., Hatzigeorgiou, A.G., and Nishikura, K. (2007). Redirection of silencing targets by adenosine-to-inosine editing of miRNAs. Science *315*, 1137–1140.
11. Borchert, G.M., Gilmore, B.L., Spengler, R.M., Xing, Y., Lanier, W., Bhattacharya, D., and Davidson, B.L. (2009). Adenosine deamination in human transcripts generates novel microRNA binding sites. Hum. Mol. Genet. *18*, 4801–4807.
12. Zhang, Z., and Carmichael, G.G. (2001). The fate of dsRNA in the nucleus: a p54(nrb)-containing complex mediates the nuclear retention of promiscuously A-to-I edited RNAs. Cell *106*, 465–475.
13. Scadden, A.D. (2005). The RISC subunit Tudor-SN binds to hyper-edited double-stranded RNA and promotes its cleavage. Nat. Struct. Mol. Biol. *12*, 489–496.
14. Morita, Y., Shibutani, T., Nakanishi, N., Nishikura, K., Iwai, S., and Kuraoka, I. (2013). Human endonuclease V is a ribonuclease specific for inosine-containing RNA. Nat. Commun. *4*, 2273.
15. Dominissini, D., Moshitch-Moshkovitz, S., Amariglio, N., and Rechavi, G. (2011). Adenosine-to-inosine RNA editing meets cancer. Carcinogenesis *32*, 1569–1577.
16. Paz, N., Levanon, E.Y., Amariglio, N., Heimberger, A.B., Ram, Z., Constantini, S., Barbash, Z.S., Adamsky, K., Safran, M., Hirschberg, A., et al. (2007). Altered adenosine-to-inosine RNA editing in human cancer. Genome Res. *17*, 1586–1595.
17. Han, L., Diao, L., Yu, S., Xu, X., Li, J., Zhang, R., Yang, Y., Werner, H.M.J., Eterovic, A.K., Yuan, Y., et al. (2015). The genomic landscape and clinical relevance of A-to-I RNA editing in human cancers. Cancer Cell *28*, 515–528.
18. Martinez, H.D., Jasavala, R.J., Hinkson, I., Fitzgerald, L.D., Trimmer, J.S., Kung, H.J., and Wright, M.E. (2008). RNA editing of androgen receptor gene transcripts in prostate cancer cells. J. Biol. Chem. *283*, 29938–29949.
19. Chan, T.H.M., Lin, C.H., Qi, L., Fei, J., Li, Y., Yong, K.J., Liu, M., Song, Y., Chow, R.K., Ng, V.H., et al. (2014). A disrupted RNA editing balance mediated by ADARs (Adenosine DeAminases that act on RNA) in human hepatocellular carcinoma. Gut *63*, 832–843.
20. Han, S.-W., Kim, H.P., Shin, J.Y., Jeong, E.G., Lee, W.C., Kim, K.Y., Park, S.Y., Lee, D.W., Won, J.K., Jeong, S.Y., et al. (2014). RNA editing in RHOQ promotes invasion potential in colorectal cancer. J. Exp. Med. *211*, 613–621.
21. Song, Y., An, O., Ren, X., Chan, T.H.M., Tay, D.J.T., Tang, S.J., Han, J., Hong, H., Ng, V.H.E., Ke, X., et al. (2021). RNA editing mediates the functional switch of COPA in a novel mechanism of hepatocarcinogenesis. J. Hepatol. *74*, 135–147.
22. Siwkowski, A.M., Malik, L., Esau, C.C., Maier, M.A., Wancewicz, E.V., Albertshofer, K., Monia, B.P., Bennett, C.F., and Eldrup, A.B. (2004). Identification and functional validation of PNAs that inhibit murine CD40 expression by redirection of splicing. Nucleic Acids Res. *32*, 2695–2706.
23. Nulf, C.J., and Corey, D. (2004). Intracellular inhibition of hepatitis C virus (HCV) internal ribosomal entry site (IRES)-dependent translation by peptide nucleic acids (PNAs) and locked nucleic acids (LNAs). Nucleic Acids Res. *32*, 3792–3798.
24. Summerton, J., and Weller, D. (1997). Morpholino antisense oligomers: design, preparation, and properties. Antisense Nucleic Acid Drug Dev. *7*, 187–195.
25. Penn, A.C., Balik, A., and Greger, I.H. (2013). Steric antisense inhibition of AMPA receptor Q/R editing reveals tight coupling to intronic editing sites and splicing. Nucleic Acids Res. *41*, 1113–1123.
26. Mizrahi, R.A., Schirle, N.T., and Beal, P.A. (2013). Potent and selective inhibition of A-to-I RNA editing with 2′-O-methyl/locked nucleic acid-containing antisense oligoribonucleotides. ACS Chem. Biol. *8*, 832–839.
27. Kaczmarek, J.C., Kowalski, P.S., and Anderson, D.G. (2017). Advances in the delivery of RNA therapeutics: from concept to clinical reality. Genome Med. *9*, 60.
28. Burns, C.M., Chu, H., Rueter, S.M., Hutchinson, L.K., Canton, H., Sanders-Bush, E., and Emeson, R.B. (1997). Regulation of serotonin-2C receptor G-protein coupling by RNA editing. Nature *387*, 303–308.
29. Niswender, C.M., Sanders-Bush, E., and Emeson, R.B. (1998). Identification and characterization of RNA editing events within the 5-HT2C receptor. Ann. N Y Acad. Sci. *861*, 38–48.
30. Fitzgerald, L.W., Iyer, G., Conklin, D.S., Krause, C.M., Marshall, A., Patterson, J.P., Tran, D.P., Jonak, G.J., and Hartig, P.R. (1999). Messenger RNA editing of the human serotonin 5-HT2C receptor. Neuropsychopharmacology *21* (2, Suppl), 82S–90S.
31. Lorenz, R., Bernhart, S.H., Höner Zu Siederdissen, C., Tafer, H., Flamm, C., Stadler, P.F., and Hofacker, I.L. (2011). ViennaRNA Package 2.0. Algorithms Mol. Biol. *6*, 26.
32. Piva, F., Giulietti, M., Burini, A.B., and Principato, G. (2012). SpliceAid 2: a database of human splicing factors expression data and RNA target motifs. Hum. Mutat. *33*, 81–85.

33. Pitt, J.M., Kroemer, G., and Zitvogel, L. (2016). Extracellular vesicles: masters of intercellular communication and potential clinical interventions. J. Clin. Invest. *126*, 1139–1143.

34. EL Andaloussi, S., Mäger, I., Breakefield, X.O., and Wood, M.J. (2013). Extracellular vesicles: biology and emerging therapeutic opportunities. Nat. Rev. Drug Discov. *12*, 347–357.

35. Usman, W.M., Pham, T.C., Kwok, Y.Y., Vu, L.T., Ma, V., Peng, B., Chan, Y.S., Wei, L., Chin, S.M., Azad, A., et al. (2018). Efficient RNA drug delivery using red blood cell extracellular vesicles. Nat. Commun. *9*, 2359.

36. Pham, T.C., Jayasinghe, M.K., Pham, T.T., Yang, Y., Wei, L., Usman, W.M., Chen, H., Pirisinu, M., Gong, J., Kim, S., et al. (2021). Covalent conjugation of extracellular vesicles with peptides and nanobodies for targeted therapeutic delivery. J. Extracell. Vesicles *10*, e12057.

37. Fumagalli, D., Gacquer, D., Rothé, F., Lefort, A., Libert, F., Brown, D., Kheddoumi, N., Shlien, A., Konopka, T., Salgado, R., et al. (2015). Principles Governing A-to-I RNA Editing in the Breast Cancer Transcriptome. Cell Rep. *13*, 277–289.

38. Maas, S., Patt, S., Schrey, M., and Rich, A. (2001). Underediting of glutamate receptor GluR-B mRNA in malignant gliomas. Proc. Natl. Acad. Sci. USA *98*, 14687–14692.

39. Jiang, Q., Crews, L.A., Barrett, C.L., Chun, H.J., Court, A.C., Isquith, J.M., Zipeto, M.A., Goff, D.J., Minden, M., Sadarangani, A., et al. (2013). ADAR1 promotes malignant progenitor reprogramming in chronic myeloid leukemia. Proc. Natl. Acad. Sci. USA *110*, 1041–1046.

40. Chan, T.H., Qamra, A., Tan, K.T., Guo, J., Yang, H., Qi, L., Lin, J.S., Ng, V.H., Song, Y., Hong, H., et al. (2016). ADAR-Mediated RNA Editing Predicts Progression and Prognosis of Gastric Cancer. Gastroenterology *151*, 637–650.e10.

41. Hong, H., An, O., Chan, T.H.M., Ng, V.H.E., Kwok, H.S., Lin, J.S., Qi, L., Han, J., Tay, D.J.T., Tang, S.J., et al. (2018). Bidirectional regulation of adenosine-to-inosine (A-to-I) RNA editing by DEAH box helicase 9 (DHX9) in cancer. Nucleic Acids Res. *46*, 7953–7969.

42. Nakano, M., Fukami, T., Gotoh, S., and Nakajima, M. (2017). A-to-I RNA Editing Up-regulates Human Dihydrofolate Reductase in Breast Cancer. J. Biol. Chem. *292*, 4873–4884.

43. Pestal, K., Funk, C.C., Snyder, J.M., Price, N.D., Treuting, P.M., and Stetson, D.B. (2015). Isoforms of RNA-Editing Enzyme ADAR1 Independently Control Nucleic Acid Sensor MDA5-Driven Autoimmunity and Multi-organ Development. Immunity *43*, 933–944.

44. Cummins, L.L., Owens, S.R., Risen, L.M., Lesnik, E.A., Freier, S.M., McGee, D., Guinosso, C.J., and Cook, P.D. (1995). Characterization of fully 2′-modified oligoribonucleotide hetero- and homoduplex hybridization and nuclease sensitivity. Nucleic Acids Res. *23*, 2019–2024.

45. Devi, G., Yuan, Z., Lu, Y., Zhao, Y., and Chen, G. (2014). Incorporation of thio-pseudoisocytosine into triplex-forming peptide nucleic acids for enhanced recognition of RNA duplexes. Nucleic Acids Res. *42*, 4008–4018.

46. Devi, G., Zhou, Y., Zhong, Z., Toh, D.F.K., and Chen, G. (2015). RNA triplexes: from structural principles to biological and biotech applications. Wiley Interdiscip. Rev. RNA *6*, 111–128.

47. Toh, D.K., Devi, G., Patil, K.M., Qu, Q., Maraswami, M., Xiao, Y., Loh, T.P., Zhao, Y., and Chen, G. (2016). Incorporating a guanidine-modified cytosine base into triplex-forming PNAs for the recognition of a C-G pyrimidine-purine inversion site of an RNA duplex. Nucleic Acids Res. *44*, 9071–9082.

48. Patil, K.M., and Chen, G. (2016). Recognition of RNA Sequence and Structure by Duplex and Triplex Formation: Targeting miRNA and Pre-miRNA. In Modified Nucleic Acids in Biology and Medicine, S. Jurga, V.A. Erdmann, and J. Barciszewski, eds. (Cham: Springer International Publishing), pp. 299–317.

49. Toh, D.K., Patil, K.M., and Chen, G. (2017). Sequence-specific and Selective Recognition of Double-stranded RNAs over Single-stranded RNAs by Chemically Modified Peptide Nucleic Acids. J. Vis. Exp. *127*, e56221.

50. Endoh, T., Hnedzko, D., Rozners, E., and Sugimoto, N. (2016). Nucleobase-Modified PNA Suppresses Translation by Forming a Triple Helix with a Hairpin Structure in mRNA In Vitro and in Cells. Angew. Chem. Int. Ed. Engl. *55*, 899–903.

51. Rozners, E. (2012). Recent advances in chemical modification of Peptide nucleic acids. J. Nucleic Acids *2012*, 518162.